19

Silver Recovery from Acidic Solutions by Formation of Nanoparticles and Submicroparticles of Ag on Microfiltration Membranes

Pilar González[1], F. Javier Recio[2], Dario Ribera[1], Oswaldo González[1], Pilar DaSilva[2], Pilar Herrasti[2] and Mario Avila-Rodriguez[1]
[1]Universidad de Guanajuato, Guanajuato
[2]Universidad Autónoma de Madrid, Madrid
[1]México
[2]España

1. Introduction

Despite environmental regulations, wastewaters generated by some industries are in some cases discharged into lakes, rivers or reservoirs after inefficient treatments or without any pretreatment for the elimination or reduction of certain pollutants. Effluents may sometimes contain valuable elements with significant commercial value such as precious metals. Recovery of these metals is important because they could be harmful to aquatic life in lakes and rivers and because of its economic value.

There are legal provisions regarding the composition of an effluent: in the case of liquids containing silver, it is a maximum of 5 ppm. It is known, however, that the silver ion could create a complex especially with thiosulfate, which has little effect on health.

Even if silver would not affect health and there were no restrictions to its discharge, there is an important reason to recover it: its value and scarcity. Annual global demand for silver is currently of 24,500 metric tons, used in a vast array of industrial and consumer products. For example, silver is widely used in industrial electroplating as a protective coating or as adornment. Silver reflects light very well, so it is used in car headlights and mirrors.

A laboratory that uses silver in its production could discharge monthly, a value of 150 to 1,800 dollars in silver.

Worldwide, approximately 57% of the silver present in discarded products is recovered. It has the highest rates of recovery among the most commonly used metals, but much of it is still lost in the various emissions to the environment.

Silver recovery

Various methodologies have been reported for the recovery of this metal ion, with efficiencies that vary depending on the experimental conditions.

Among the most common methods for silver recovery are: 1) Metal Replacement; 2) Electrolytic Recovery; 3) Precipitation; 4) Distillation; 5) Ion Exchange and 6) The use of

new compounds to precipitate silver (soil, silica, clays, etc.). The main features of the first five are:

1. Metal Replacement. It is one of the most popular and economical methods. It consists of a cartridge containing iron, wool and wooden chips or spirals. A solution circulates with a constant flux through the cartridge. As the silver is removed, iron is depleted, producing sediment. Finally the sediment is refined to recover the silver. One cartridge recovers 90% of silver, two in a series, 95%. Although the cost of implementation is low, the cost of refining is higher than the value of the recovered silver.
2. Electrolytic recovery. This technology was introduced in the year 1930. It uses a cell with two electrodes immersed in a solution, to which a constant current is applied. The silver is reduced to pure metal on the cathode (usually stainless steel). There are two basic types of this technic: one where the cathode rotates in a solution and another where the solution flows around the cathode. The recovery is around 96% (20 to 60 grams/ hour of high purity) and it is easy to operate.
3. Precipitation. It was the first practical method for silver recovery. It has been used for over 50 years, so it is highly developed. It also precipitates copper, cadmium, mercury, lead, nickel and tin, amongst other metals. It uses a precipitant together with a flocculating agent to increase the size of the particles. Silver is recovered by filtration and then refined, with a yield of 99%. However, the equipment and the precipitant are expensive.
4. Distillation. It is normally used together with the external management of effluents. It reduces the amount of liquid to be transported:80 to 100% of water could be removed, leaving thick or solid silver. With this method 99% of silver could be recovered. The cost is high and it is recommended almost exclusively for industrial laboratories.
5. Ion Exchange. This technology can be used in solutions that have low percentages of silver, like stabilizers or wash water. In this process the metallic silver is obtained through a reversible process in which ions are exchanged between a solid (resin) and water with ionized salts. With a single column more than 90% of the silver could be recovered. With two columns in a series, about 99% could be recovered.

None of these methods gives any importance to the size or shape of the recovered metallic silver particles. Their main interest is on the efficiency of the recovery process. The recovery of the silver in specific shapes and sizes (nano and submicrometric), is an added value of the recovery processes.

1.1 Nanoparticles

Although nanomaterials have always existed in nature, our understanding of their properties and how they influence their environment has been limited. Many of these materials are currently under study and their applications have been developed over the last two decades.

Their manufacturing has gained importance because of their unusual properties compared to bulk materials. Examples include aluminium nanoparticles of 20 to 30 nm which can spontaneously combust while bulk aluminium is stable (Gromov & Vereshchagin, 2004) and calcium carbonate that forms either a fragile chalk or tough abalone shells, depending on the structural arrangement of the molecules (Tong-Xiang et al., 2009).

The applications of this relatively new technology are large and include: conductive plastics (Aravind et al., 2003), anticorrosive coatings (Gangopadhyay & De, 2000), fuel cells and batteries (González-Rodriguez, 2007; Ponce de León, 2006), solar energy generation

(Granqvist, 2007; Bavykin & Walsh, 2010), electricity carriers (Conte et al., 2004), fire resistant materials (Hamdani et al., 2010), computing and data storage (Jimenez & Jana, 2007), sensors (Yun et al., 2008; Rivas et al. 2009), water treatment (Thavasi et al., 2008), catalysis (Cheng et al., 2010) and early identification of cancer cells (Nanomedicine, 2007). Although many of these applications still remain untested, the investment over the last few years has been large: the USA allocated more than a billion dollars in 2005 (Pedreño A., 2005), and more recently Japan and the European Union invested 770 and 1400 million euros, respectively in scientific programs involving nanomaterials (EU Official Website, 2010).
Among the metallic nanomaterials, silver has been intensively studied because of its wide applications including catalysis, electronics, photonics, and photography (Maillard et al., 2010). Furthermore, low-dimensional silver materials may be utilized as interconnectors or as active components in the manufacture of micro/ nanodevices (Sun et al., 2002).

1.1.1 Synthesis of silver nanomaterials

Many reports have focused on the synthesis of shape controlled Ag nanostructures, including quasi-spheres, decahedrons, cubes, prisms, rods, wires, tubes, branches, sheets or plates, and belts (Yin et al., 2001; Du et al., 2007; Cobley et al., 2009). Generally, size-controlled Ag particles can be realized adjusting the reaction parameters. Evanoff and Chumanov synthesized Ag particles with diameters between 15 and 200 nm, through variations in the reaction time (Evanoff & Chumanov, 2004). By varying the concentration of sodium borohydride ($NaBH_4$) employed in the reaction, Metraux and Mirkin have provided a straight forward and rapid route to Ag nanoprisms withover prism thickness control (Metraux & Mirkin, 2005). By adjusting intensity and spectral properties of the irradiating light, Pietrobon and Kitaev synthesized decahedral Ag nanoparticles with controllable regrowth to larger sizes (Pietrobon & Kitaev, 2008). Also, Yin's laboratory has recently demonstrated that the aspect ratio and optical properties of Ag nanoplates can be tuned with precision, over a wide range through a UV-light-induced reconstruction process (Zhang et al., 2009). However, in these examples of qualitative size control, the results can only be roughly speculated before the experiment (e.g., size-decrease or increase, but with no precise measurement). Quantitative size-control, where the product is size-designed by adjusting the reaction conditions to produce the desired particle sizes predictably and accurately, has not yet been established. Actually, it is well-known that the chemical synthesis of metal nanocrystals is influenced by several thermodynamic and kinetic factors, and much difficulty remains in capturing the distinct stages of nucleation and growth of nanocrystals (Burda et al., 2005). Also, it is very hard to establish a quantitative function to describe the relationship between the synthesis conditions and the size of the product. Therefore, carrying out qualitative and especially quantitative synthesis of size-controlled Ag particles is still a great challenge.
The synthesis of silver nanoparticles has been studied searching for an easy control over kinetics. The preparation of the conditions for each of the methods mentioned above, play an important role on the composition, structure and size of nanoparticles, and have a direct impact on their properties. The development of a methodology to provide adequate control of particle size in a simple way is an important contribution to the synthesis.
This paper presents a novel approach to recovering silver from aqueous solutions in its most valuable form: the metallic and the formation of particles with different size depending on the experimental conditions. This includes the reduction of silver ions with a reducing agent such as ascorbic acid in a microfiltration system. During reduction of the silver ions, the membrane is used as a support for the metallic silver formed. The size and shape of the

nanoparticles depends on different parameters such as, silver, nitric and ascorbic acids concentrations and the stirring rate of the solutions. Considering the extensive applications of nano and submicrometer Ag particles as catalysts, conductive adhesives, display devices, passive components, inkjet printing, photon emission, and higher order multiples resonances substrates (Dai et al., 2011; Hu et al., 2010; Xu et al. 2008; Sung et al., 2010; Gloskowskii et al., 2008), this methodology could be used in a wide range of industrial applications.

2. Experimental

2.1 Methodology for the transference of Ag (I)

All products used had analytical grade and were used as received. The device used for this work is shown in Figure 1 and comprises a two-compartment cell, divided by a microfiltration membrane.

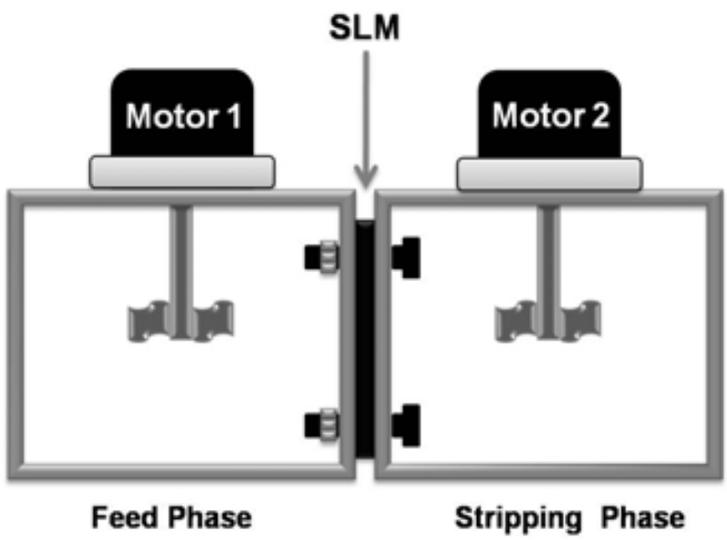

Fig. 1. Cell used for the recovering of silver, the membrane is located in between the two compartments

The feed phase was composed by different concentrations of $AgNO_3$ (from 25 to 100 mg L^{-1}) at various HNO_3 concentrations (from 0.1 to 1 mol L^{-1}). The stripping phase was composed by a solution of ascorbic acid and its concentrations were changed from 0.2 to 1.5 mol L^{-1}. The feed and stripping solutions were added to compartments 1 and 2, respectively. The cell was then covered and the system was stirred. Aliquots were taken from both sides at several different times and, finally; Ag (I) content was analyzed by atomic flame absorption using a Perkin-Elmer Analyst 200 flame atomic absorption spectrometer. The pH of both the feed and stripping solutions was measured with the help of a combined glass electrode using a Methrom potentiometer (Titrino 716). The ascorbic acid's quantitative determination in both compartments was performed by Iodometry using a standard solution of iodine and starch as an indicator of endpoint.

The microporous membrane used, was a polyvinylidene difluoride (PVDF) hydrophilic membrane with 75% porosity, 125 μm thickness and average pore size of 0.22 μm (Millipore). During reduction of the silver ions, the membrane is used as a support for the metallic silver formations.

After every experiment, the membrane was removed from the system and the water was eliminated by evaporation. Subsequently, the membrane was weighed to determine the variation with respect to its initial weight.

The characterization of the metallic silver particles was carried out with a SEM (Scanning Electronic Microscope) Hitachi S-3000N coupled to an EDAX InCAx-sight analyzer. Contact angle of the microporous membrane with ascorbic acid solutions and Ag (I) in HNO_3 solutions was measured using the CAM 200 from KSV Instruments Ltd. This unit has a measuring range of 0° to 180°, with an uncertainty of ± 0.1°.

3. Results and discussion

3.1 Silver nanoparticles formation on the microfiltration membranes

The recovery of Ag (I) was carried out using Ag^+ 100 mg L^{-1} and HNO_3 0.25 mol L^{-1} as the feed solution, and a solution of ascorbic acid (HA) 1 mol L^{-1} as the stripping solution. The contact time of the membrane with the feed and stripping solutions was 30 minutes, with a stirring speed of 600 rpm at both compartments.

After 30 minutes, the membrane was removed from the cell. The side of the membrane in contact with the feed solution showed a deposit, while any deposits were observed on the face in contact with the stripping solution. Figure 2a shows a part of the microfiltration membrane that was in contact with the feed solution. Figure 2b corresponds to an image obtained with the optical microscope.

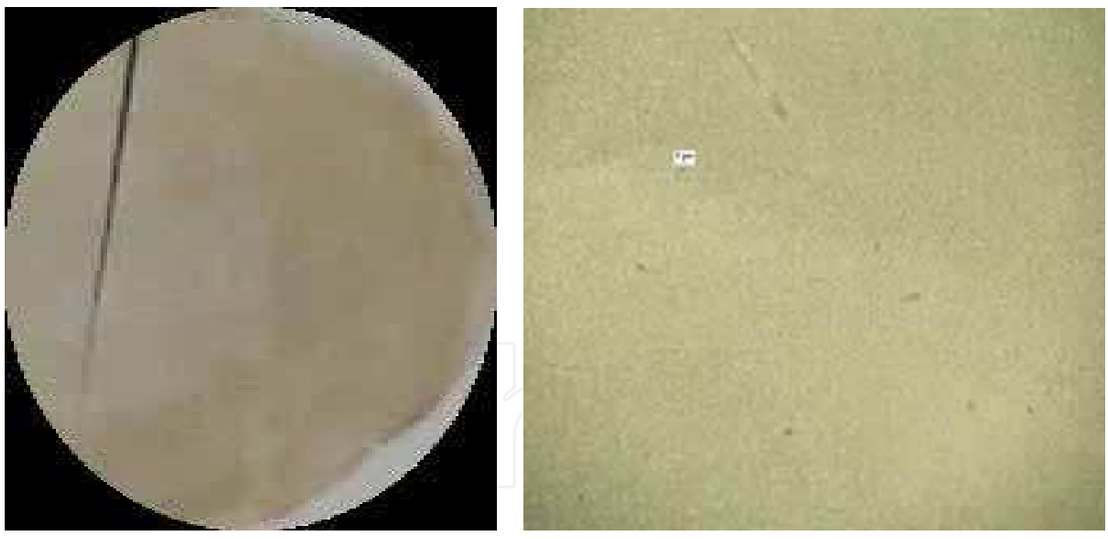

(a) (b)

Fig. 2. Images of (a) microfiltration membrane after contact with the feed (Ag (I)) and stripping (HA) solutions; and (b) small part of the membrane through an optical microscope

This deposit may have been caused by the formation of metallic silver by the reduction of Ag (I) with ascorbic acid. The deposit seems uniform both to the naked eye and through the optical microscope. In addition, the formation of silver on the membrane is consistent with the decrease concentration of Ag^+ ions in the feed solution (see Figure 3). No concentration of Ag^+ was detected in the stripping solution.

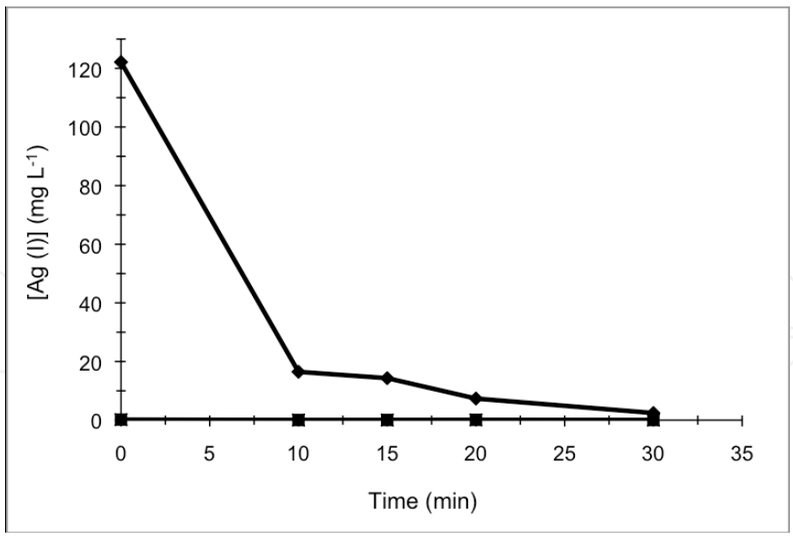

Fig. 3. Variation of Ag (I) concentration as a function of time. (◆)Feed solution: [Ag(I)] = 100 mg L^{-1}; [HNO_3] = 0.25 mol L^{-1}. (■) Stripping solution: [HA] = 0.25 mol L^{-1}

Comparing the weight of the membrane before (m1 = 0.1447 g) and after the experiment (m2=0.1739 g), we found that the difference in weigh was 29.2 mg. While the initial concentration of Ag+ ions in the feed solution was 122 mg L^{-1} and the volume of both solutions was 250 mL, for each trial, the amount of metallic silver that could be deposited on the membrane is of 30.5 mg. This value is very close to the mass in excess of the membrane and it corresponds to the metallic silver deposited on the membrane. The yield of silver recovery in these conditions is around 96%. To confirm the presence of metallic silver on the membrane, an EDAX analysis was performed. Figure 4 shows the spectrum which indicates the peaks that correspond to metallic silver.

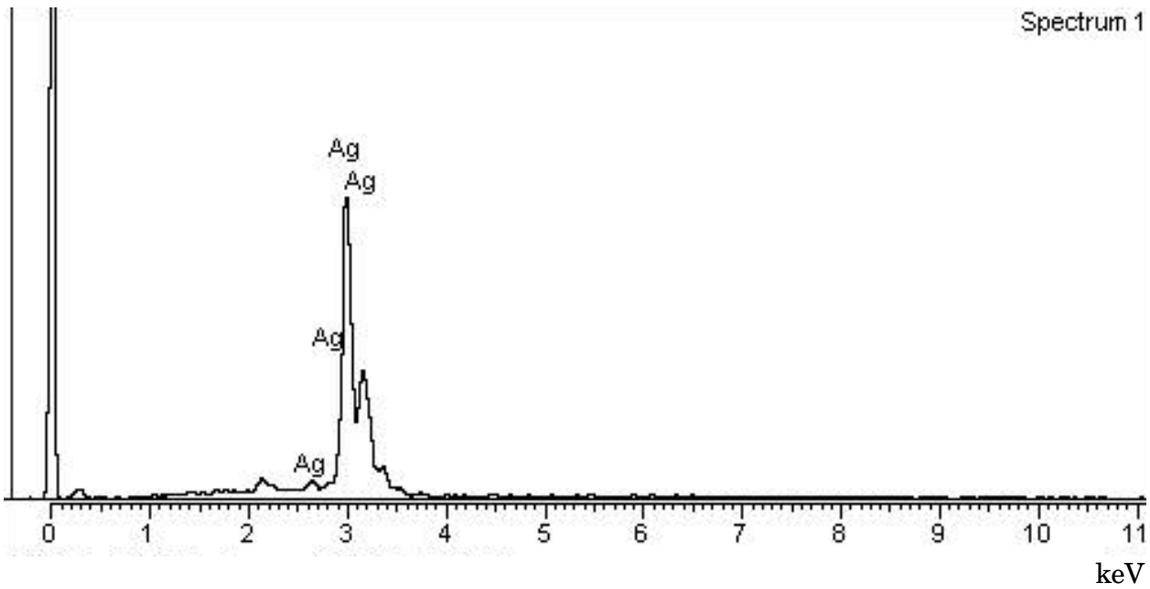

Fig. 4. EDAX spectrum of the membrane after contac twith the feed (Ag (I)) and stripping (HA) solutions

A deeper more detailed analysis on the morphology of the deposits was carried out using Scanning Electron Microscopy (SEM). The micrographs of different membranes are shown in Figure 5. The silver particles formed, are distributed over the membrane and in its pores. The shape acquired by the metallic silver depends on the synthesis conditions. We observe a non-homogeneous 3D growth, with a hexagonal shape resemblance and a broad size distribution. A similar result was recently reported by Masaharu et al., 2010.

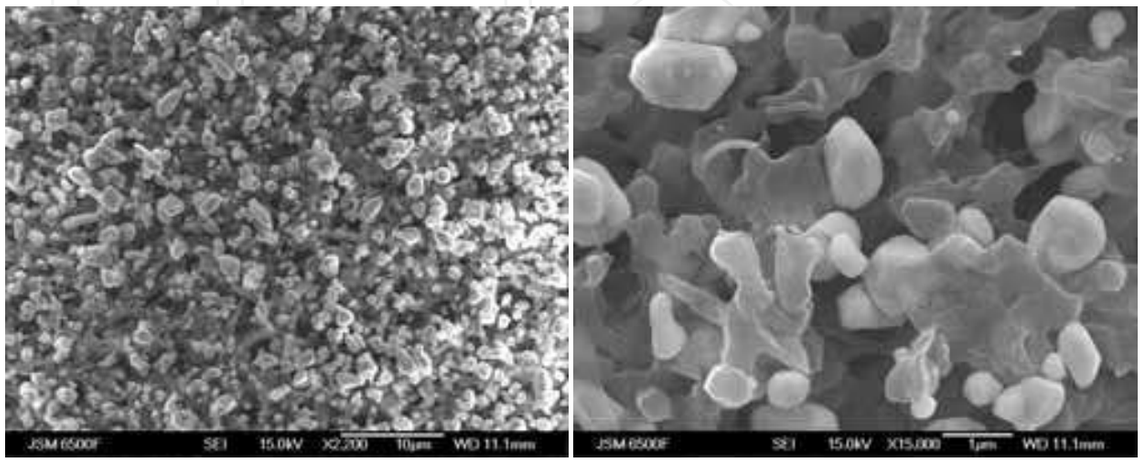

(a) (b)

Fig. 5. Micrograph of the silver particles on the membrane. Feed solution: 100 mg L^{-1} of Ag (I). Stripping solution: [HA] = 1 mol L^{-1}. Stirring speed: 600 rpm at both compartments. (a) and (b) are the same sample with different magnification

It is also evident, that the stirring speed has an impact on the size and location of the particles (on the surface or in the pores of the membrane). Figure 6 shows the micrographs of silver particles deposited on the microfiltration membrane at different stirring speeds.

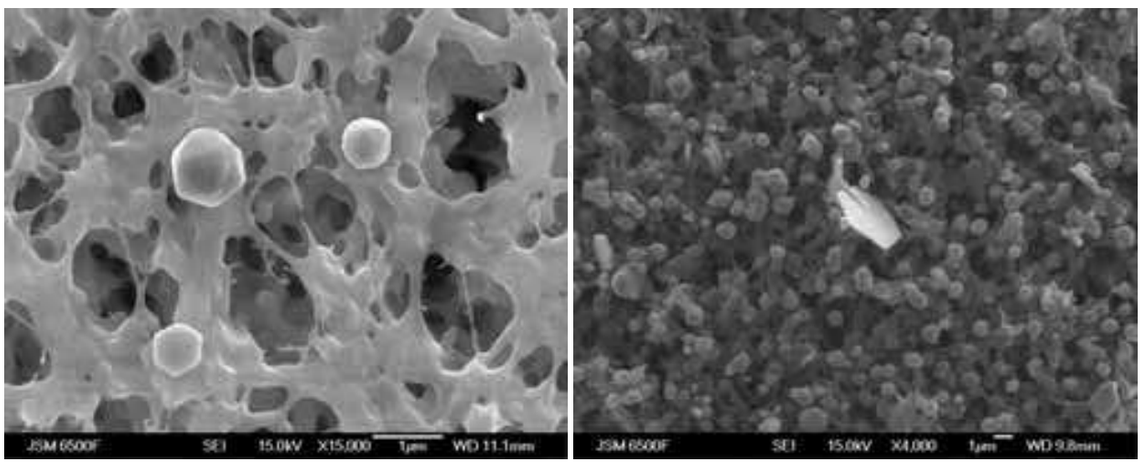

(a) (b)

Fig. 6. Micrograph of silver particles on the membrane, same solution that in figure 5.
(a) stirring speed 300 rpm, at both compartments. (b) stirring speed 1200 in the feed solution and 800 rpm in the stripping solution

As in the previous conditions, the silver particles are distributed over the membrane. For a stirring speed of 350 rpm at both phases, the silver particles shape is well defined, showing a hexagonal 3D growth (figure 6a and 6b). For a higher stirring speed (Figure 6c and 6d), the shape of the silver particles is less homogeneous. As we will show later in this paper, the crystalline shapes of the silver particles are highly dependent on the nucleation speed and are based on hydrodynamic and chemical aspects. The hexagonal crystal plate shape has been reported earlier in the literature (Jixiang et al., 2007; Masaharu et al. 2010).

Figure 7 shows the micrographs of silver particles deposited on the microfiltration membranes when a low stirring speed (350 rpm) or no agitation is applied to the stripping solution and different stirring speeds applied to the feed solution. From this, it is clear that every stirring speed causes significant changes in the shape and size distribution of the silver particles. For a 350 rpm stirring speed in the stripping solution (to 600 rpm in the feed

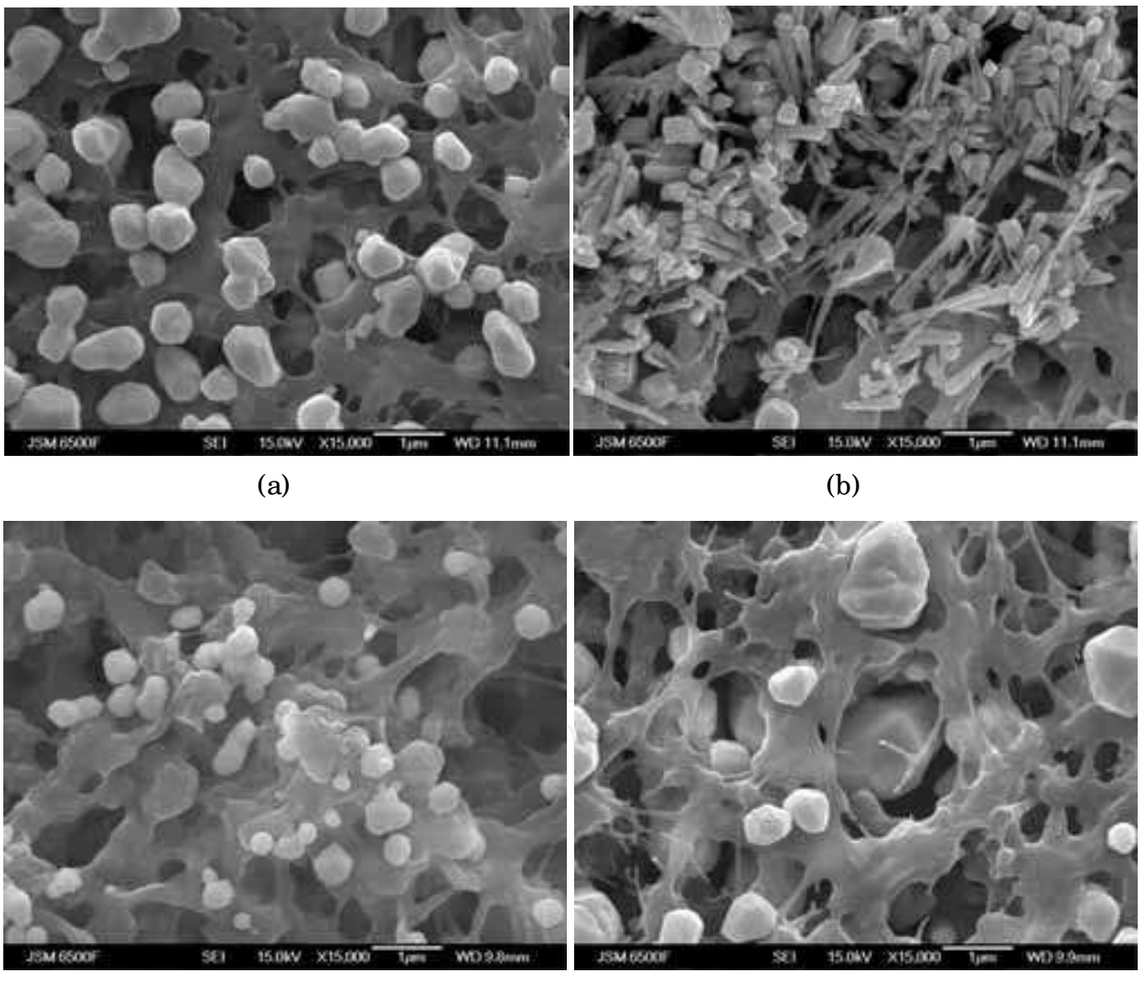

(a) (b)

(c) (d)

Fig. 7. Micrograph of silver particles on the membrane obtained with different stirring speeds in the two compartments. (a) Stirring speed 350 rpm in the stripping solution and 600 rpm in the feed solution. (b), (c) and (d) No agitation of the stripping solution. To the feed solution a stirring speed of 1000, 600 and 300 rpm, is applied respectively

solution), the particles maintain a certain homogeneity. A decahedron shape is observed in figure 7a. On the other hand, when the stripping solution was not stirred and the stirring speed on the feed solution was reduced (1000, 600, 300 rpm) the shape of the silver crystals gets very different. In the case of a stirring speed of 1000 rpm, the metallic silver takes crystal morphology in the shapes of cubes and rods. If the stirring speed is decreased to 600 rpm, the silver particles appear as rounded shapes but with traces of nucleation that form a cubic shape (figure 7b, 7c). At 300 rpm on the feed solution, the silver particles take decahedron shapes with an average particle size greater than in other cases. Also in this case, the large silver particles are occluded in the pores of the microfiltration membrane. It is important to observe that the proposed methodology is very suitable for obtaining metallic silver particles of different shapes and sizes. In fact, in the literature, in order to obtain different shape and size silver nanoparticles, more controlled and drastic conditions are required than those proposed here.
Finally, in the absence of stirring at both phases, the silver particles obtained on the membrane surface, clearly show the formation of hexagonal plates (Figure 8). These hexagonal plates come from the formation of dendrites on the surface, which is the first stage in the process of crystallization of silver on the microfiltration membrane.

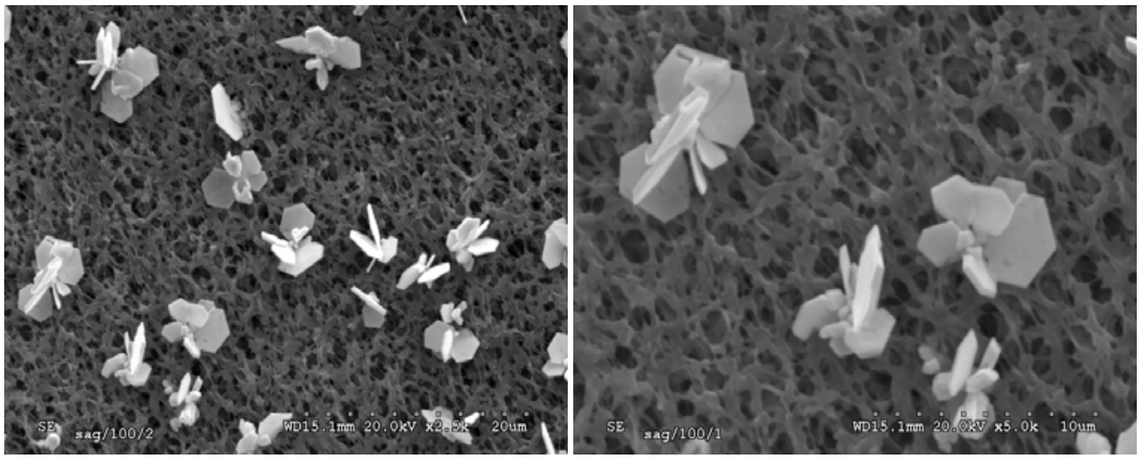

(a) (b)

Fig. 8. Micrograph of the silver particles on the membrane when no stirring is applied to the solutions. (b) Higher magnification of the same sample

We can conclude that hydrodynamics play an important role in the morphology and size of silver particles.
In the next section we will discuss the chemical aspects that affect the process of reducing Ag^+ ions by ascorbic acid. Additionally, we will analyze the conditions for efficient recovery of silver so we will have a better understanding of the mechanism under which the process is under mass transfer of Ag^+ ions.

3.2 Effect of Ag (I)'s concentration on the recovery efficiency

In order to evaluate the influence of Ag(I)'s concentration on the efficiency recovery of the proposed separation system, two tests with different concentrations of Ag(I) (25 and 100 mg L^{-1}), were performed. For the first test we used a 0.25 mol L^{-1} of HNO_3 as the feed solution

and 1 mol L^{-1} of ascorbic acid as the stripping solution. Figure 9 shows the variation of C_t/ C_o with the Ag (I) in the feed solution as a function of time (being C_o the initial concentration of Ag (I) and C_t the concentration at time t).

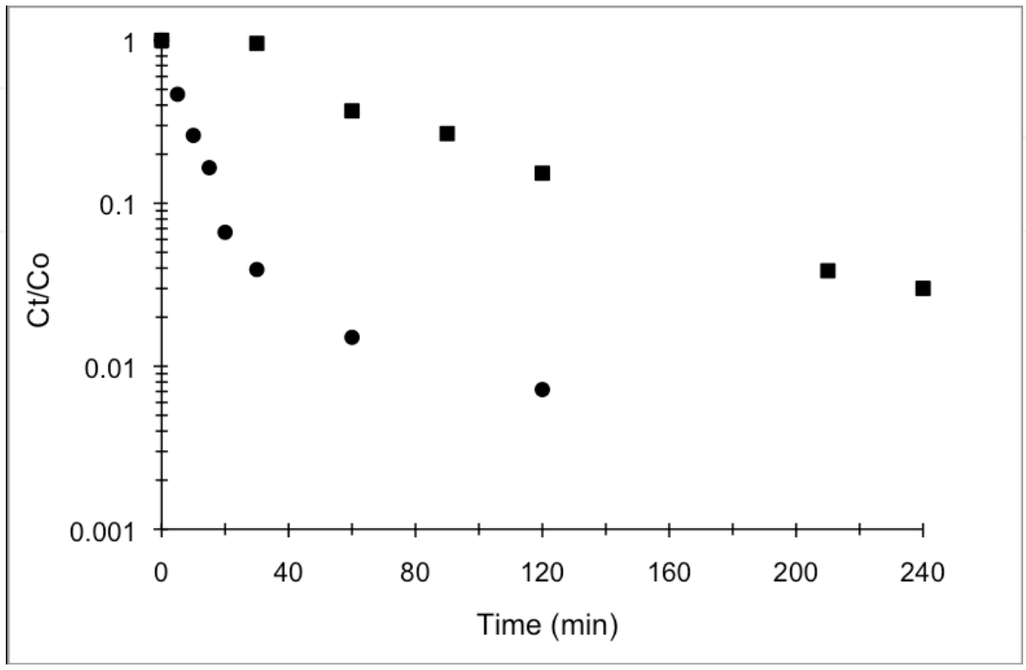

Fig. 9. Silver's C_t/ C_o variation in the feed solution as a function of time. (■) [Ag (I)] = 25 mg L^{-1};(●)[Ag (I)] = 100 mg L^{-1}. Stripping solution [HA] = 1 mol L^{-1}

Silver C_t/ C_o values decrease as function of time, in the feed solution in both tests. Silver recovery efficiency is near 95%. For initial silver's concentration of 25 and 100 mg L^{-1}, the recovery efficiency is 99%. Silver's concentrations decrease faster when the initial concentration is 100 mg L^{-1}. The concentration of Ag (I) in the stripping solution was practically negligible after 120 minutes of contact (no more than 0.2 mg L^{-1}). Therefore, we can consider that the transfer of Ag (I) from the feed solution to the stripping solution is negligible. In both cases the membrane has a silver deposit on the surface in contact with the feed solution, so that the absence of silver ions in the feed solution is due to its reduction induced by the ascorbic acid.

When a 25 mg L^{-1} concentration of silver is used in the feed solution, the quantity of silver particles on the surface of the membrane, are scarce and show a less uniform distribution (data not shown). Nevertheless, the silver particles morphology is quiet similar to the observed previously, namely in decahedra shapes.

3.3 Effect of the H^+ ions' and the ascorbic acid's concentrations

The effect of H^+'s concentration in the reduction of silver by ascorbic acid and its deposition on the microfiltration membrane, was performed by varying the HNO_3 concentration between 0 (pH 5) to 1 mol L^{-1} into the feed phase, while the ascorbic acid concentration was 1 mol L^{-1} into the stripping phase. The stirring speed was kept constant, in both compartments, at 600 rpm. In all cases the experimental time was 120 minutes. The recovery efficiency was evaluated by analyzing the amount of Ag (I) in the feed and in stripping

solutions as a function of time. Figure 10 shows the micrographs obtained in each condition. Figure 10a shows a dendritic shape of the silver particles when no HNO_3 is added to the solution. When HNO_3 is added to the feed solution, the particles have a decahedral structure (figures 9b, 9c, 9d); like those obtained earlier. Another important observation is that when the nitric acid's concentration increases, the number and size of silver particles on the membrane decreases. The shape in all cases does not change very much. In the absence of HNO_3 acid, the feed solution becomes cloudy after 5 minutes, suggesting that the Ag (I) reduction process takes place not only in the feed solution membrane interface but also in the bulk of the feed solution. By increasing the H^+'s concentration in the feed solution, the solution does not become cloudy and the silver is reduced on the membrane. The size distribution and dispersion of these particles is higher at 0.5 mol L^{-1} (Figure 9c) than at 0.1 mol L^{-1} (Figure 9b) of nitric acid. When the concentration of H^+ is increased to 1 mol L^{-1} (Figure 9d), there are few particles left on the membrane, indicating that a decrease in pH acts negatively on the Ag(I) reduction process, decreasing the reduction rate and generating fewer and smaller particles on the membrane.

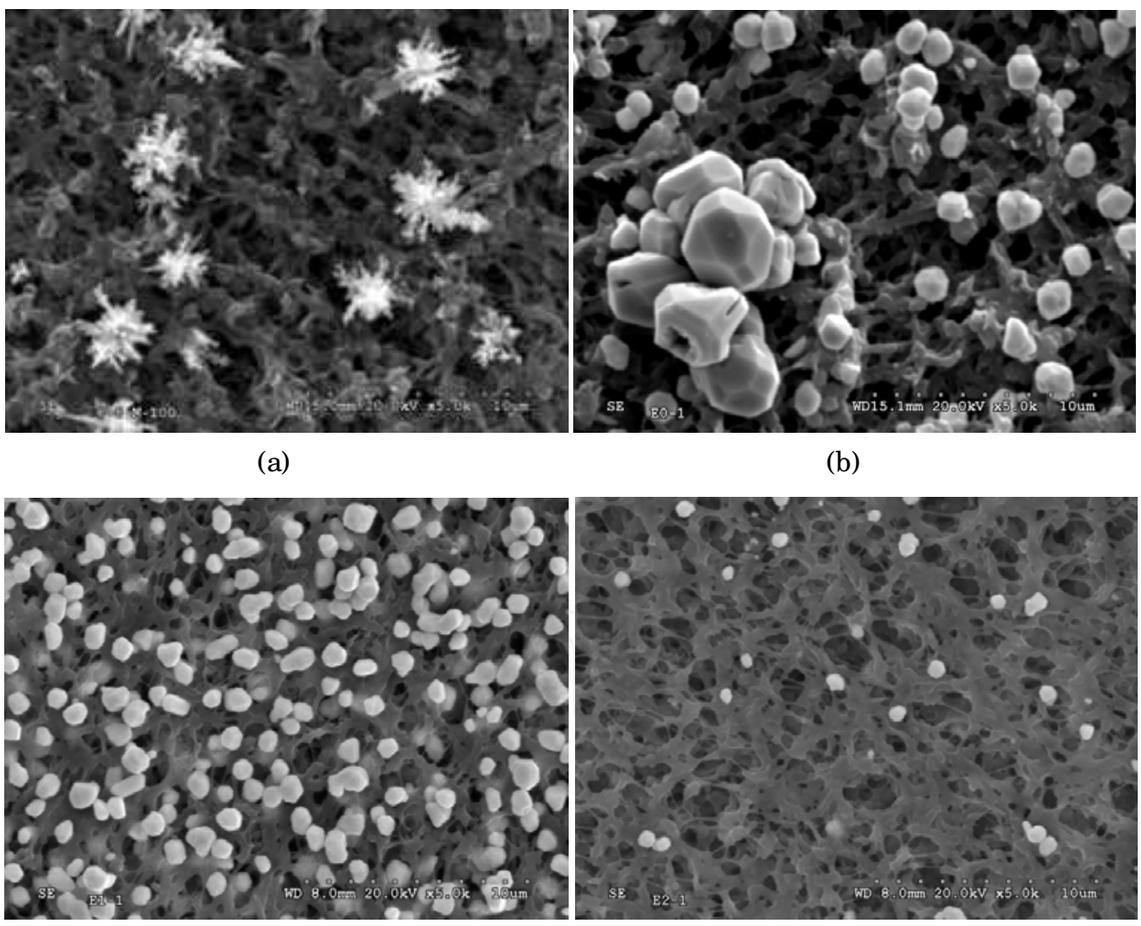

(a) (b)

(c) (d)

Fig. 10. Micrographs of the membrane after 120 minutes of contact. Feed solution: [Ag(I)] = 100 mg L^{-1}, [HNO_3]: a) without, pH 5.4, b) 0.1 mol L^{-1}, c) 0.5 mol L^{-1} and d) 1 mol L^{-1}. Stripping solution: [HA] =1 mol L^{-1}

Figure 11 shows the morphology of the silver nanoparticles at different HNO_3's concentration in the feed solution when the ascorbic acid concentration is reduced from 1 mol L^{-1} to 0.5 mol L^{-1} in the stripping solution. The silver deposits obtained, show a similar morphology that in Figure 10. The only difference is the amount of reduced silver; in this case the amount is less. In the absence of HNO_3, the morphology of the particles is dendritic (Figure 11a), but in the presence of HNO_3 acid a decahedra structure was obtained (Figure 11b, 11c and 11d). A more uniform particle size and better distribution occurs at low concentrations of acid in the feed compartment.

From this study it was found that a greater amount of ascorbic acid increases the reduction of Ag (I) on the membrane. The increase of H^+'s concentration results in a reduced amount of silver but on a more uniform shape and size.

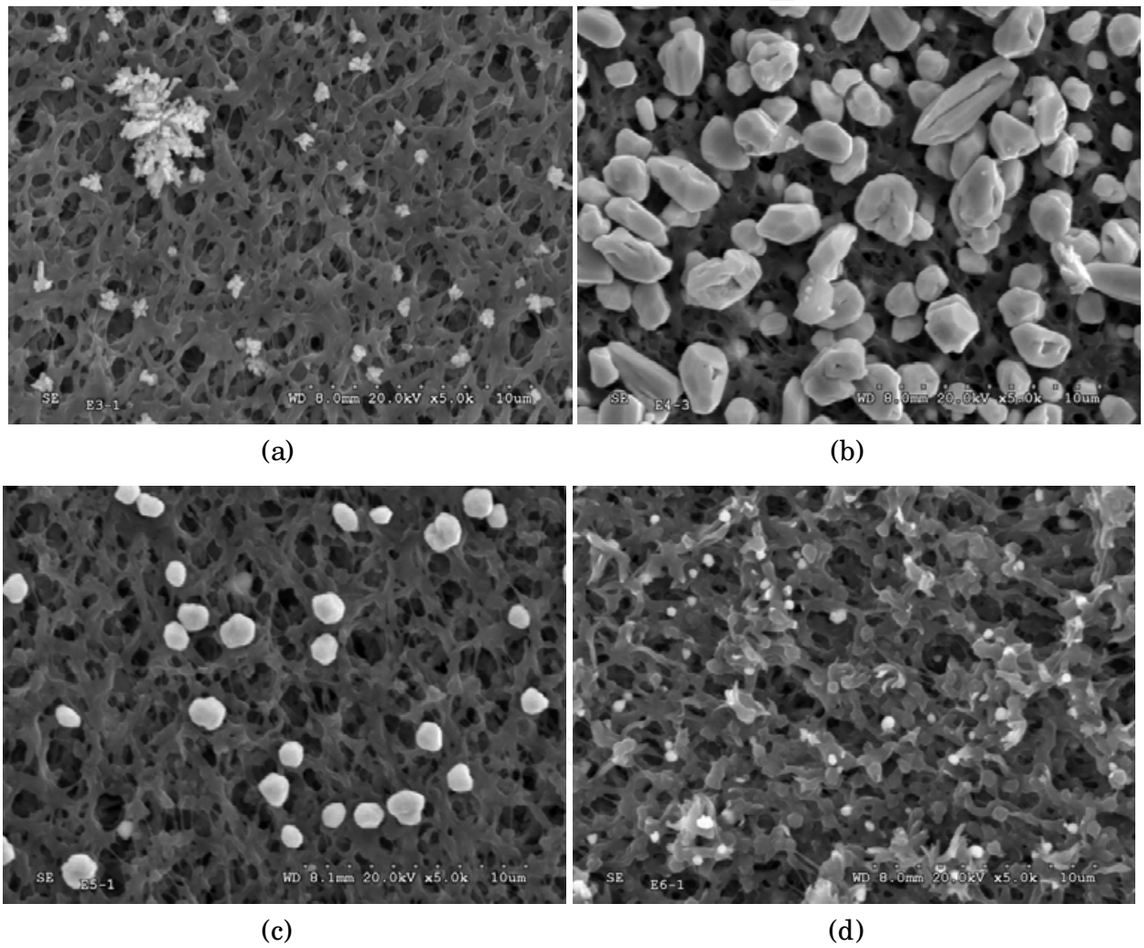

(a) (b)

(c) (d)

Fig. 11. Micrographs of the membranes after 120 minutes of contact. Feed solution: [Ag^+] = 100 mg L^{-1}; [HNO_3]: a) without, pH 5.4, b) 0.1 mol L^{-1}, c) 0.5 mol L^{-1} and d) 1 mol L^{-1}. Stripping solution: [HA] = 0.5 mol L^{-1}

3.4 Analysis of the mass transfer process of Ag (I)

The morphology of Ag particles obtained is directly related to the hydrodynamic and chemical conditions of the system proposed. But also, the morphology is connected with the

mass transfer process of Ag^+ ions from the feed solution towards the specific zone where the redox process takes place with the ascorbic acid (which is also transported from the stripping solution).

The analysis of the concentration profiles of [Ag^+] at different concentrations of HNO_3 in the feed phase and with a two different ascorbic acid's concentrations in the stripping phase, allows to see that the rate of decrease of [Ag^+] in the feed solution as a function of time (figures 12a and 12b), strongly depends on the conditions of the feed phase as much as those of the stripping phase.

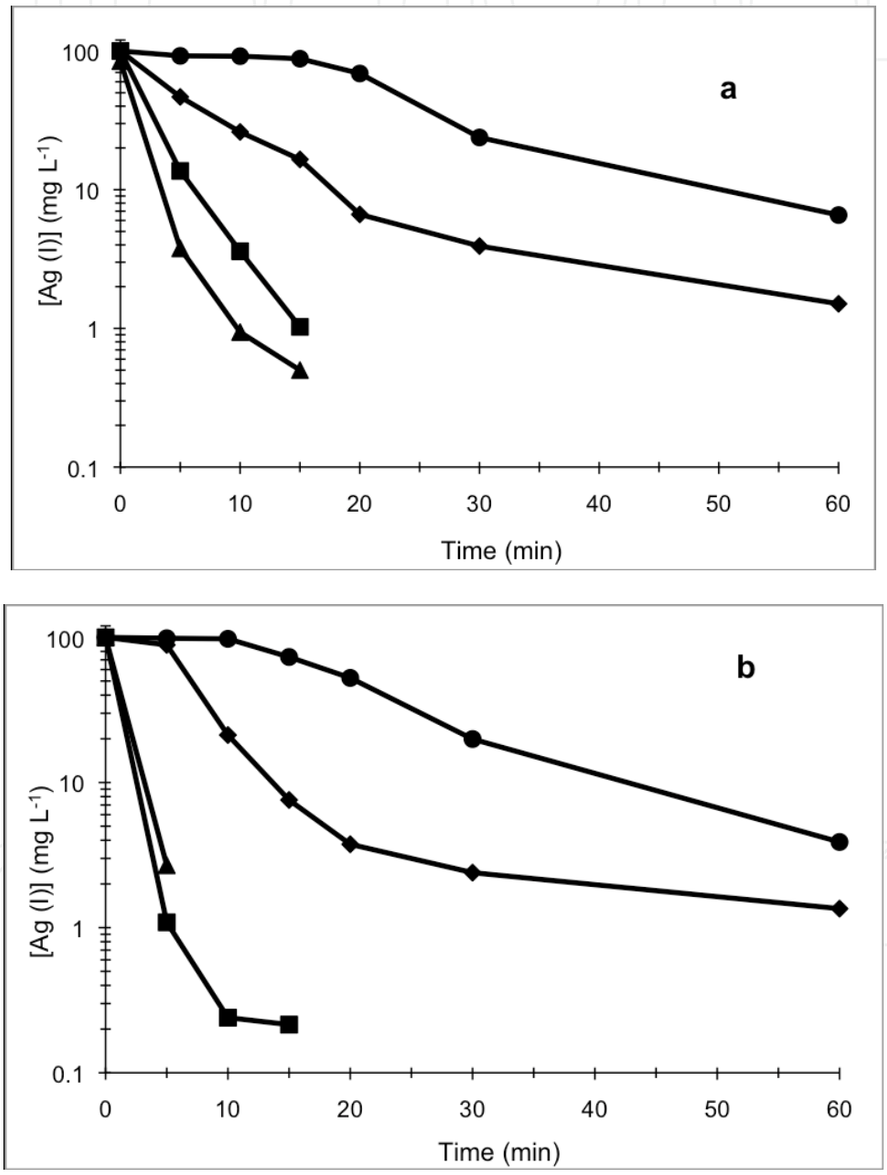

Fig. 12. Variation of Ag (I) concentration as a function of time in the feed compartment for different nitric acid's concentrations. (▲) In the absence of HNO_3, pH = 5.4; (■) [HNO_3] = 0.1 mol L^{-1}; (◆) [HNO_3] = 0.5 mol L^{-1}; (●) [HNO3] = 1 mol L^{-1}. Stripping solution: (A) [HA] = 1 mol L^{-1}, (B) [HA] = 0.5 mol L^{-1}

With a higher pH (without a HNO_3 addition) at the feed phase, we reach the highest Ag reduction rate, as shown in figure 12A. Due to the low Ag^+ concentration found at the stripping phase after the test, the Ag^+ mass transfer through the microfiltration membrane cannot be considered during the reduction process, indicating that the redox process takes place inside of the microfiltration membrane. Final Ag^+ concentrations in the feed solutions are close to 2% of the initial value, indicating a high yield process.

When the pH in the feed phase is 5, the $[Ag^+]$ in the feed solution diminishes to less than 1%, and a precipitate becomes apparent in the feed solution. This one can be associated to the saturation of Ag precipitate in the membrane and due to the stirring process the Ag particles come to the feed solution. However, when pH is reduced in the feed solution, the Ag precipitated in the feed solution does not appear anymore and all the Ag particles are retained in the membrane. When the HNO_3 concentrations are higher than 0.5 mol $L^{-1,}$ the reduction rates are slow and the curves trends of $[Ag^+]$ remain constant during the first 30 minutes of the experiment.

To explain the results obtained it is necessary to analyse the various phenomena that take place at the membrane. There are two important aspects: 1) Ag^+ and HA mass transfer process, and 2) the redox process of both compounds connected with the formation of silver particles.

In analysing the mass transfer process of Ag^+ and HA, it is necessary to consider the different zones existing in the system. Close to the membrane, a non-stirring zone exists. In non-stirring areas Ag^+ and HA movements are controlled by a diffusion process because the convection process is negligible. Figure 13 shows the several areas formed due to the stirring process. Zones named *a)* and *e)* correspond to non-stirring areas (diffusion region) in feed and stripping phases. Zones named *b)* and *d)* represent the interphases feed-membrane phase and stripping-membrane phase respectively, and *c)* is the membrane phase. The thickness of the diffusion regions are represented by d_a and d_e, corresponding to the thickness of feed and stripping diffusion areas respectively and d_o is the membrane thickness.

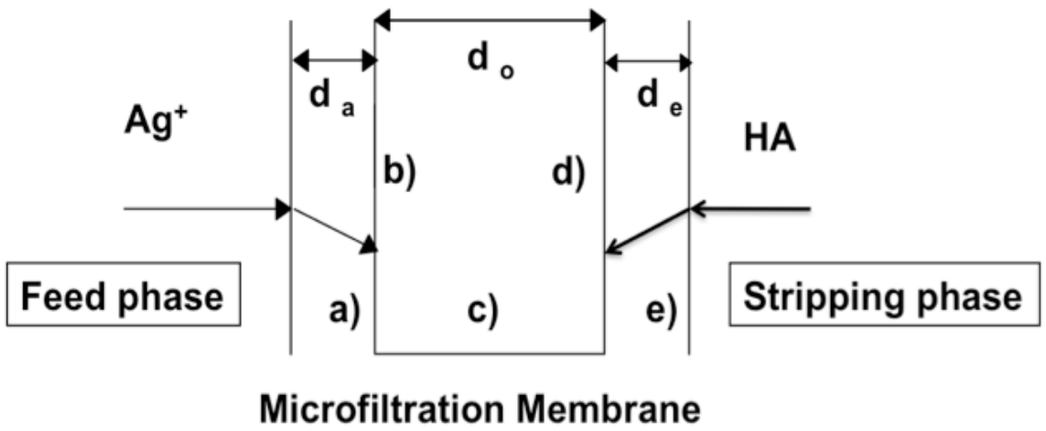

Fig. 13. Scheme of the mass transfer of Ag (I) and ascorbic acid (HA)

In order to correctly define the mass transfer process, it is necessary to determine the areas where the redox process could take place. The experimental results show that the redox process takes place mainly at the feed-membrane interface and Ag particles are formed on the feed side of the membrane. Based on this result, the Ag^+ and HA mass transfers were studied in the absence of one of the two compounds, alternately Ag^+ mass transfer studies

were performed by replacing HA by different concentrations of HNO_3 at the stripping phase (pH from 0 to 5), and a feed solution of Ag (I) 100 mg L^{-1} and HNO_3 0.5 mol L^{-1}. The Ag^+ concentration in the stripping phase after all the experiments, shows values around 10%, indicating that Ag^+ diffusion through the stripping phase is very low in all tests performed. A pH decrease in the stripping phase is also detected and this effect is more pronounced when the initial pH in the stripping phase is higher. Figure 14 shows Ag^+ concentrations in both phases.

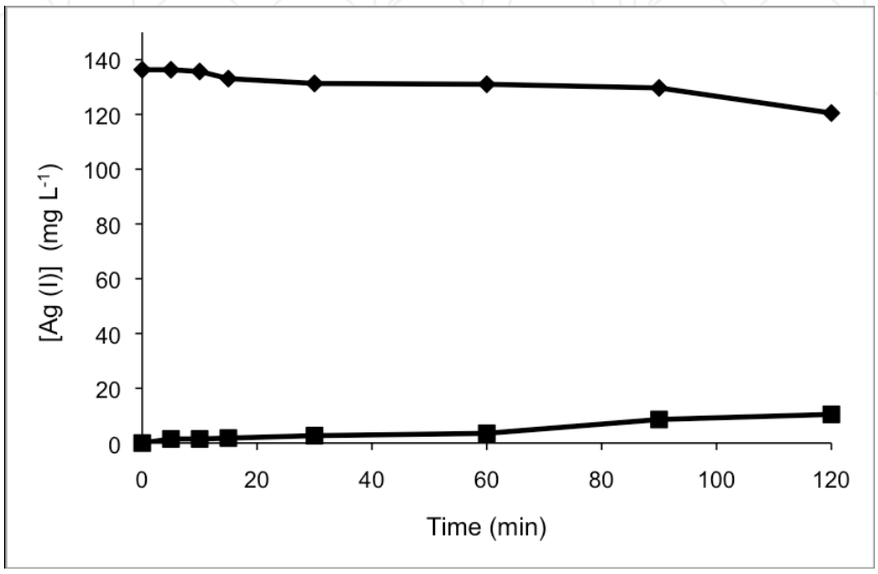

Fig. 14. Variation of Ag (I) concentration as a function of time in absence of HA. (◆) Feed solution: [Ag (I)] = 100 mg L^{-1}; [HNO_3] = 0.5 mol L^{-1}. (■) Stripping solution: [HNO_3] = 1 mol L^{-1}

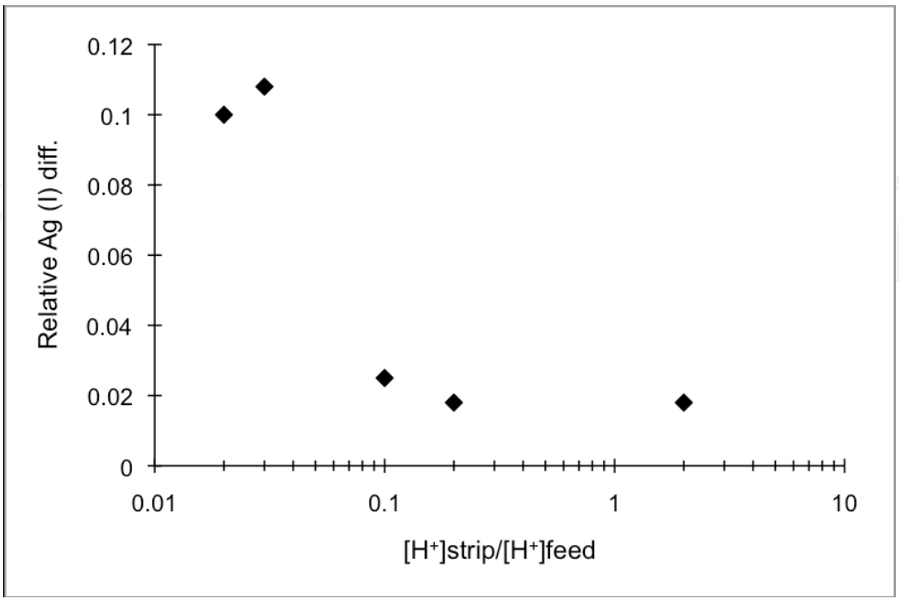

Fig. 15. Relative Ag^+ (I)'s concentration as a function of [H^+]strip/ [H^+]feed

Analyzing the value of H^+'s concentration in the feed and in the stripping solutions, we found that there is a proton transfer from the feed solution to the stripping solution due to a concentration gradient. The silver ions diffused to the stripping compartment are related with the H^+ transfer. The diffusion of Ag^+ increases with the increasing of the H^+'s concentration in the feed solution. This effect can be observed in Figure 15.

The transference of ascorbic acid trough the membrane has been studied using a feed solution containing HNO_3 at different concentrations (0.1, 0.25 y 0.5 mol L^{-1}) and a HA's concentration of 1 mol L^{-1} in the stripping solution. The results show that the concentration of ascorbic acid in the feed phase after 120 minutes is minimal for each of the conditions studied. Figure 16 shows the results of the transfer of HA through the microfiltration membrane when HNO_3 in the feed solution was 0.5 mol L^{-1}.

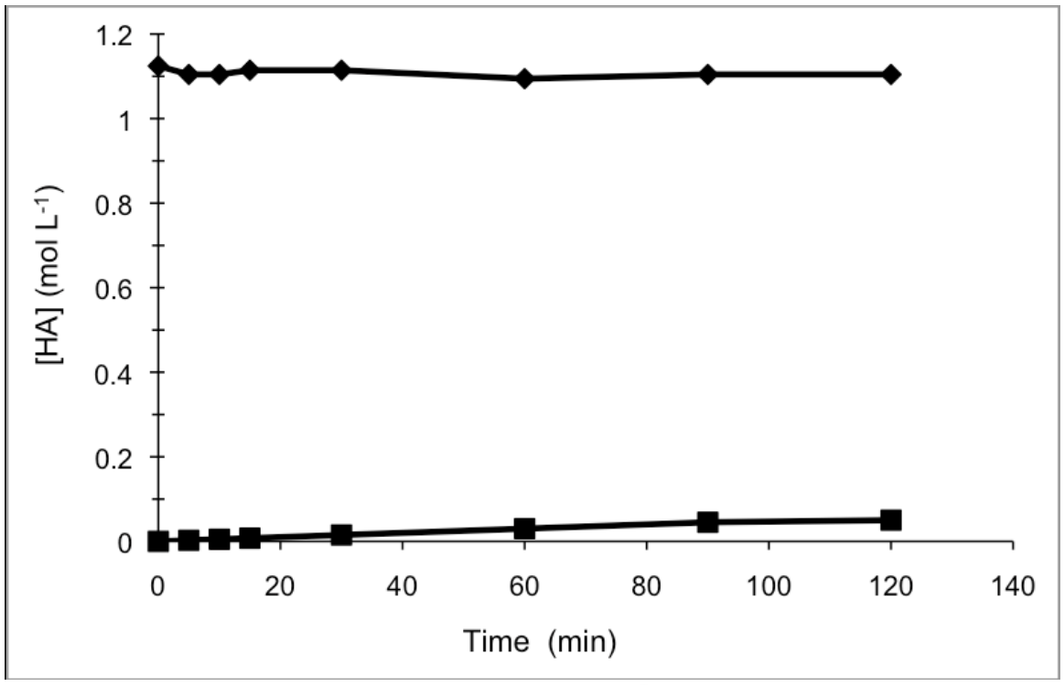

Fig. 16. Variation of the ascorbic acid's concentrations in the stripping (◆) and feed (■) phases as a function of time

In summary both Ag^+ and HA have a minimum transfer through the microfiltration membrane. This behavior can be explained considering that the membrane is made of a polyvinylidene fluoride polymer whose surface has been modified to increase the hydrophilicity. This modification produces electrical charges on the membrane surface. These charges could be positive or negative depending on the nature of aqueous solutions that are in contact with the membrane. Thus, there may be a rejection of the membrane to the charged species present in the interface membrane/ feed or membrane/ stripping solution. Although no transfer occurs of any of both species through the membrane, we have shown that the oxireduction reaction takes place in the interface (feed solution/ membrane) generating silver nanoparticles on the membrane.

In order to determine the degree of rejection of the microfiltration membrane to Ag^+ and ascorbic acid, contact angle measurements were performed. Table 1 shows the contact angle

for a PVDF hydrophilic membrane and as means of comparison we included a PVDF hydrophobic membrane.

	PVDF Hydrophobic / H_2O	PVDF Hydrophilic/ H_2O	PVDF Hydrophilic/ $AgNO_3$ / HNO_3 0.1 mol L^{-1}	PVDF Hydrophilic/ $AgNO_3$ / HNO_3 0.5 mol L^{-1}	PVDF Hydrophilic/ HA
Contact angle (°)	143.1	72.9	115.2	114.58	58.47

Table 1. Contact angle values of the microfiltration membrane in contact with water and solutions containing $AgNO_3$ (100 mg L^{-1})/ HNO_3 and ascorbic acid 1 mol L^{-1}

It can be seen that the values of water contact angles on a hydrophobic PVDF membrane are higher than those obtained with a hydrophilic PVDF membrane. When the polarities are very close, the contact angles are smaller. Also the analysis of Table 1 shows that the contact angle values of the solutions of Ag^+ are higher than those obtained with solutions of HA and water, and are similar to the contact angle values of a hydrophobic membrane with water (large difference in polarity). This clearly indicates that there is a rejection of the membrane to the $AgNO_3$/ HNO_3 solutions.

Analyzing the variation of the contact angle as a function of time (see Table 2), we found that in the case of solutions $AgNO_3$/ HNO_3 the value of the contact angle after 6 seconds, remained around 114º. In the case of ascorbic acid, the value of the contact angle ranged from 50.48º to 58.47º, which is a considerable variation. The decrease in the contact angle value indicates that the membrane gets impregnated by the ascorbic acid. Thus, the HA is transported into the membrane to reach the interfacial membrane area, where the oxireduction reaction is carried out.

Time (s)	$AgNO_3$ 100 mg L^{-1} HNO_3 0.5 mol L^{-1} Contact angle (°) (Average)	HA 1 mol L^{-1} Contact angle (°) (Average)
1.00	114.58	58.47
2.00	113.29	55.17
3.00	114.09	53.66
4.00	114.29	52.41
5.00	114.64	51.51
6.00	114.11	50.48

Table 2. Contact angle values of a microfiltration membrane in contact with water and solutions containing $AgNO_3$ (100 mg L^{-1})/ HNO_3 and ascorbic acid 1 mol L^{-1} as a function of time

According to the above, the formation process speed of silver nanoparticles depends on the diffusion speed of Ag^+ ions to the membrane. If this speed is lower than the oxidation-

reduction speed, the diffusion process takes place and it is possible to calculate the overall mass transfer coefficient of the Ag^+ using the equation (1).

$$Ln\frac{[Ag^+]_t}{[Ag^+]_0} = -K\frac{Q}{V}t \quad (1)$$

Where:
K = overall mass transfer coefficient
t = time (sec)
Q = effective area of the membrane (11.34 cm^2)
V = volume (250 cm^3)
The overall mass transfer coefficient depends on the diffusion rate as well as on the chemical reaction between silver ions and ascorbic acid.
The variation of Ln $[Ag^+]_t/ [Ag^+]_0$ as a function of t*Q/ V, is a straight line with a slope equal to –K. Figure 17 shows the results obtained in the case of a system containing a feed solution of Ag(I) 100 mg L^{-1} with different HNO_3 concentrations and 1 mol L^{-1} of HA in the stripping solution.

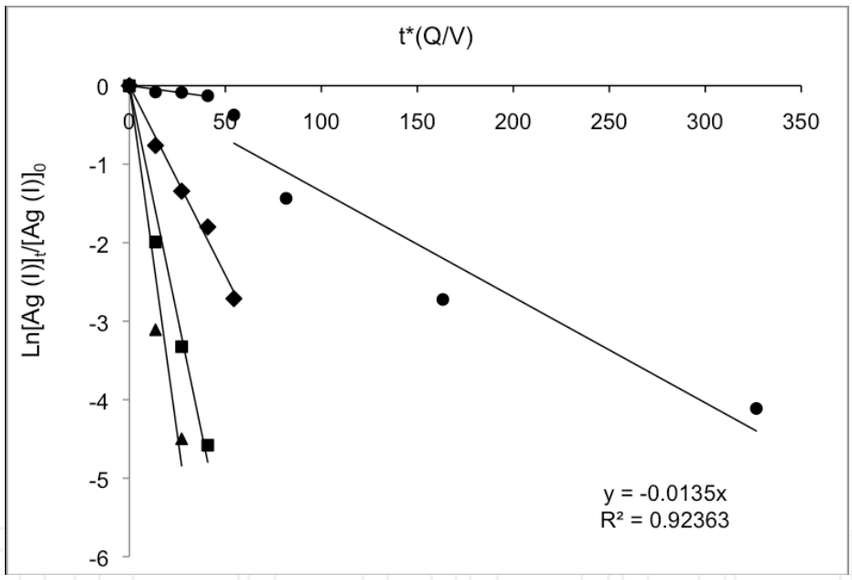

Fig. 17. Variation of de Ln$[Ag^+]_t/ [Ag^+]_0$ as function of t*Q/ V in the feed compartment for different nitric acid's concentrations. (▲) Without HNO_3, pH = 5.4; (■) $[HNO_3]$ = 0.1 mol L^{-1}; (◆) $[HNO_3]$ = 0.5 mol L^{-1}; (●) $[HNO_3]$ = 1 mol L^{-1}. Stripping solution: [HA] = 1 mol L^{-1}

The value of K (slope) obtained for the system in absence of HNO_3 is 0.1779 cm s^{-1},with a R^2 value of 0.94. For a HNO_3 concentration of 0.1 mol L^{-1}, in the feed solution, the value of K (0.1175 cm s^{-1}) is very close to the former. In these two cases the K values are high for a system with a diffusion control. It is important to note that under these conditions, the formation of silver nanoparticles not only occurs in the feed phase-membrane interface but also in the bulk of the feed solution, then the process is controlled by the redox reaction. On the other hand, when the concentration of HNO_3 is 0.5 mol L^{-1}, the value of the overall mass transfer coefficient is 0.0483 cm s^{-1}. When the HNO_3's concentration is 1 mol L^{-1}, there are

two well-defined zones, one with a value for K of 0.0033 cm s^{-1} and another with an overall mass transfer coefficient of 0.0135 cm s^{-1}. It is clear that an increase of the HNO_3's concentration, has a negative effect on the speed of the oxireduction reaction between Ag^+ ions and HA. Moreover, to understand better the results shown in Figure 17, it is necessary to consider the rate of impregnation of the membrane by HA. In the absence of HNO_3, the rate of impregnation of the membrane by the HA, appears to be faster than in the acidic media. This is why the K value diminishes with the increase of HNO_3's concentration and at 1 mol L^{-1} of HNO_3, the variation of $[Ag^+]$ remains almost constant during the first 30 minutes of contact between the phases and the membrane (Figure 12a and 12b).

It is possible to correlate the values of the global mass transfer coefficient with the morphology of silver particles deposited in the microfiltration membrane under each of the studied conditions. When the ascorbic acid rapidly permeates the microfiltration membrane (low concentration of HNO_3 in the feed solution) the value of K is high (0.1779 cm s^{-1}). The silver particles obtained in this case, have a dendritic shape (figure 10a and 11a). If the value of K decreases, the silver crystals grow as decahedra (Figures 10b and 11b). Finally, the no agitation of the feed and stripping phases make transference process very slow, and under these conditions the crystallization time is sufficient for the formation of metallic silver hexagonal plates (figure 8). These observations agree with those reported in the literature regarding the process of crystallization of metallic silver, which in a first stage involves the formation of dendrites trees that slowly form decahedra shaped particles leading to the formation of hexagonal plates (Jixiang et al. 2007).

The methodology proposed is suitable for obtaining silver nanoparticles and submicroparticles on microfiltration membranes with different shapes and sizes. The control of mass transference can be carried out by changes in the stirring solutions, the pH, and the concentrations of Ag^+ and ascorbic acid. The conditions used in this methodology are not drastic being an advantage over other methods reported.

4. Conclusions

We have developed a methodology for the recovery of silver (I) from aqueous solutions on a microfiltration membrane using ascorbic acid as a reducing agent. Under certain conditions, it is possible to recover about 99% of the silver contained in the aqueous solutions. The silver particles are deposited in nanometric and submicron sizes. The shape of these particles depends on the hydrodynamic and chemical conditions of the system. Silver particles can be obtained as dendrites, decahedra and hexagonal plates. We have analyzed the mass transfer process of the species involved in the system in order to explain the observed phenomena and to correlate the morphology of the particles obtained, with the mass transfer process. We can conclude that the reaction between silver and ascorbic acid occurs at the interface membrane-feed solution. The permeation rate of ascorbic acid into the membrane is linked to the Ag^+ mass transfer process. Finally, the global coefficient of mass transfer is related to the morphology of the particles obtained. At high K values, silver dendrites nanoparticles are obtained; whereas if the value of K decreases the deposit of silver particles corresponds to a slow crystallization process. The methodology proposed allows the efficient recovery of Ag (I) ions and allows the obtaining of microfiltration membranes modified by Ag particles, which can be used as filters for the removal of microorganisms contained in water.

5. Acknowledgments

The authors gratefully acknowledge the financial support of the Universidad de Guanajuato, Mexico and Spanish Ministry through the project MAT2009-14741-C02-02. Oswaldo Gonzalez would like to thank CONACYT for financial support.

6. References

Aravind D., Zhong-Zhen Y., Yiu-Wing M. (2009). Electrically conductive and super-tough polyamide-based nanocomposites. *Polymer*, 50, 4112-4121. ISSN: 0032-3861.

Bavykin D.V., Walsh F.C. (2010). Titanate and Titania Nanotubes; Synthesis, Properties and Applications. RSC Publishing, Cambridge, UK. *Nanoscience & Nanotechnology*. ISSN: 1550-7033.

Burda C., Chen X., Narayanan R.,. El-Sayed M.A, (2005). Chemistry and properties of nanocrystals of different shapes. *Chem. Rev* 105, 1025-1102. ISSN: 0009-2665.

Cheng F., Su Y., Liang J., Tao Z., Chen J. (2010). MnO_2-based nanostructures as catalysts for electrochemical oxygen reduction in alkaline media. *Chem. Mater*. 22 (3) 898-905. ISSN: 0897-4756.

Cobley C., Rycenga M., Zhou F., Li Z., Xia Y., (2009) Etching and growth: An intertwined pathway to silver nanocrystals with exotic shapes. *Angew. Chem., Int. Ed.* 48, 4824-4827 ISSN: 1521-3773.

Conte M., Prosini P.P,Passerini S (2004). Overview of energy/ hydrogen storage: state-of-the-art of technologies and prospects for nanomaterials. *Mat. Sci. Eng. B-Solid* 108, 2-8. ISSN: 0921-5107.

Dai Y.M., Pan T.C., Liu W.J., Lehng J.M. (2011). Highly dispersed Ag nanoparticles on modified carbon nanotubes for low-temperature CO oxidations. *Applied catalysis B-Environmental.* 103, 221-225. ISSN: 0926-3373.

Du J., Han B., Liu Z., Liu Y., Kang D., (2007). Control synthesis of silver nansheets, chainlike sheets and microwires via a simple solvent-thermal method. *Cryst. Growth Des.* 7, 900-904. ISSN: 1528-7505.

Evanoff D.D, Chumanov G., (2004) Size-controlled synthesis of nanoparticles. 1. "silver only" aqueous suspensions via hydrogen reduction. *J Phys. Chem. B* 108, 13948-13956 ISSN: 1089-5647.

Gangopadhyay R., De A. (2000). Conducting polymer nanocomposites: A Brief Overview. *Chem. Mater*. 12, 608-622. ISSN: 0897-4756.

Gloskowskii A., Valdaitsev D.A., Cinchetti M., Nepijko, S.A., Lange J., Aeschlimann M., Bauer M., Klimenkow M., Viduta L.V., Tomchuk P.M., Schonhense G. (2008). Electron emission from films of Ag and Au nanoparticles excited by a fentosecond punm-probe laser. *Physical Review B.* 77, Article number: 195427. ISSN: 1095-3795.

Gonzalez-Rodriguez J.G., Lucio-Garcıa M.A., Nicho M.E., Cruz-Silva R., Casales M., Valenzuela E. (2007). Improvement on the corrosion protection of conductive polymers in pemfc environments by adhesives. *J Power Sources* 168, 184-190. ISSN: 0378-7753.

Granqvist C.G. (2007). Transparent conductors as solar energy materials: A panoramic review. *Sol. Energ. Mat. Sol. Cells*. 91, 1529-1598. ISSN: 0927-0248.

Gromov A., Vereshchagin V. (2004). Study of aluminum nitride formation by superfine aluminum powder combustion in air. *J Eur. Ceram. Soc*, 24 2879-2884. ISSN: 0955-2219.

Hamdani S., Longuet C., Perrin D., Lopez-Cuesta J.M, Ganachaud F. (2009). Flame retardancy of silicone-based materials. *Polymer Degrad. Stab.* 94, 465-495. ISSN: 0141-3910.

Hu A., Guo J.Y., Alariji H., Patane G., Zhou Y., Compagnini G., Xu C.X. (2010). Low temperature sintering of Ag nanoparticles for flexible electronics packaging. *Applied Physics Letters*. 97, Article number: 153117. ISSN: 1077-3118.

Jimenez G.A, Jana S.C. (2007). Electrically conductive polymer nanocomposites of polymethylmethacrylate and carbon nanofibers prepared by chaotic mixing. *Composites Part A: Applied Science and Manufacturing*, Volume 38, Issue 3, March 2007, Pages 983-993. ISSN: 1359-835X.

Jin R., Cao Y., Mirkin C.A., Kelly K.L., Schatz G.C., J. Zheng, (2001). Photoinduced conversion of silver nanospheres to nanoprisms. *Science*, 294, 1901-1903. ISSN: 1095-9203.

Jixiang F., Hongjun Y., Peng K., Yan Y., Xiaoping S., Bingjun D. (2007). Silver Dendritic Nanostructure Growth and Evolution in Replacement Reaction. *Crystal Growth & Design*, Vol 7, No. 5, 864. ISSN: 1528-7505.

Maillard M., Giorgio S., Pileni M.P, (2003) Tuning the size of silver nanodisks with similar aspect ratios: synthesis optical properties. *J Phys. Chem.*, 107, 2466-2470. ISSN: 0022-3654.

Masaharu Tsuji, Masatoshi Ogino, Ryoichi Matsuo, Hisayo Kumagae Sachie, Hikino, Taegon Kim, Seong-Ho Yoon (2010). Stepwise Growth of Silver Nanocrystals *Crystal Growth & Design*, Vol 10, No. 1, 296. ISSN: 1528-7505.

Metraux G.S., Mirkin C. A., (2005). Rapid thermal synthesis of silver nanoprisms with chemically tailorable thickness. *Adv. Mater* 17, 412. ISSN: 1521-4095.

Nanomedicine. National Horizon Scanning Unit Emerging Technology Bulletin. Published by HealthPACT Secretariat Department of Health and Ageing, (February 2007). Available at http:/ / www.horizonscanning.gov.au [accessed September 2010].

Official website of the United States National Nanotechnology Initiative
http:/ / www.nano.gov [accessed September 2010].

Pedreño A. Nanotecnología y nanociencia: Aspectos económicos.
http:/ / iei.ua.es/ nanotecnologia [accessed September 2010].

Pietrobon B., Kitaev V., (2008). Photochemcial synthesis of monodisperse size-controlled silver decahedral nanoparticles and their remarkable optical properties *Chem. Mater*. 20, 5186-5190 ISSN: 0897-4756.

Ponce de León C., Bavykin D.V., Walsh F.C. (2006). The oxidation of borohydride ion at titanate nanotube supported gold electrodes. *Electrochem. Comm.* 8, 1655-1660. ISSN: 1388-2481.

Rivas G.A., Rubianes M.D., Pedano M.L., Ferreyra N.F., Luque G., Miscoria S. A. (2009). Carbon Nanotubes: A New Alternative for Electrochemical Sensors. *Nova Science Publishers*. 978-1-60741-314-1. ISSN: 1535-6698.

Sun Y., Gates B., Mayers B., Xia Y.. Crystalline silver nanowires by soft solution processing (2002). *Nano Lett.* 2, 165-168. ISSN: 1530-6984.

Sung D., Vornbrock A.D., Subramanian V. (2010). Scaling and optimization of gravure-printed silver nanoparticle lines for pinted electronics. *IEEE Transaction of components and packaging technologies*. 33, 105-114. ISSN: 1521–3331.

Thavasi V., Singh G., Ramakrishna S. (2008). Electrospun nanofibers in energy and environmental applications. *Energ. Environ. Sci*. 1, 205-221. ISSN: 1754-5692.

Tong-Xiang F., Suk-Kwun Ch., Di Z. (2009). Biomorphic Mineralization: From Biology to Materials, *Progress in Materials Science*, 54(5): 542-659. ISSN: 0079-6425.

Xu J., Fu C., Li Y.C. (2008). Self-bank metal conductor fabricated with silver nanoparticles. *Journal of the Society for information display*. 16, 599-602. ISSN: 1071-0922.

Yun Y., Dong Z., Shanov V.N, Doepke A., Heineman W.R, Halsall H.B., Bhattacharya A, Wong D.K.Y, Schulz M.J (2008). Fabrication and characterization of carbon nanotube array electrodes with gold nanoparticles tips. *Sensors and Actuators B: Chemical*, Volume 133, Issue 1, July 2008, Pages 208-212. ISSN: 0925-4005.

Zhang Q., Ge J., Pham T., Goebl J., Hu Y., Lu Z., Yin Y., (2009) Reconstruction of Ag Nanoplates by UV Irradiation: Tailored Optical Property and Enhanced Stability. *Angew. Chem., Int. Ed.* 48, 3516-3519 ISSN: 1521-3773.

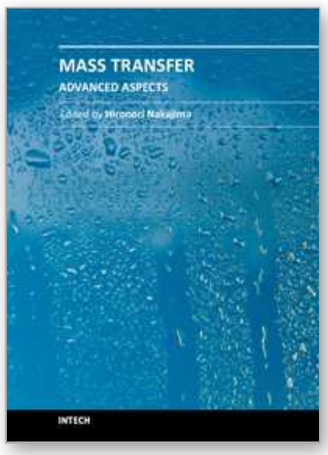

Mass Transfer - Advanced Aspects

Edited by Dr. Hironori Nakajima

ISBN 978-953-307-636-2
Hard cover, 824 pages
Publisher InTech
Published online 07, July, 2011
Published in print edition July, 2011

Our knowledge of mass transfer processes has been extended and applied to various fields of science and engineering including industrial and manufacturing processes in recent years. Since mass transfer is a primordial phenomenon, it plays a key role in the scientific researches and fields of mechanical, energy, environmental, materials, bio, and chemical engineering. In this book, energetic authors provide present advances in scientific findings and technologies, and develop new theoretical models concerning mass transfer. This book brings valuable references for researchers and engineers working in the variety of mass transfer sciences and related fields. Since the constitutive topics cover the advances in broad research areas, the topics will be mutually stimulus and informative to the researchers and engineers in different areas.

InTech Europe
University Campus STeP Ri
Slavka Krautzeka 83/A
51000 Rijeka, Croatia
Phone: +385 (51) 770 447
Fax: +385 (51) 686 166
www.intechopen.com

InTech China
Unit 405, Office Block, Hotel Equatorial Shanghai
No.65, Yan An Road (West), Shanghai, 200040, China
中国上海市延安西路65号上海国际贵都大饭店办公楼405单元
Phone: +86-21-62489820
Fax: +86-21-62489821

IntechOpen